Eur. Phys. J. B **33**, 133–145 (2003)
DOI: 10.1140/epjb/e2003-00150-3

THE EUROPEAN PHYSICAL JOURNAL B

Cycloidal vortex motion in easy-plane ferromagnets due to interaction with spin waves

A.S. Kovalev[1], F.G. Mertens[2,a], and H.J. Schnitzer[2]

[1] Institute for Low Temperature Physics and Engineering, 47 Lenin Ave., 61103, Kharkov, Ukraine
[2] Physikalisches Institut, Universität Bayreuth, 95440 Bayreuth, Germany

Received 9 December 2002
Published online 4 June 2003 –

Abstract. The dynamics of a non-planar vortex in a two-dimensional easy-plane ferromagnet of finite size is studied. Spin dynamics simulations show small cycloidal oscillations of the vortex around its mean path. In contrast to an earlier phenomenological theory we give a physical explanation: The oscillations occur due to the interaction of the vortex with coherent spin waves which are excited by this vortex at the moment when it starts to move, in order to conserve the total energy and angular momentum. The calculation of these quantities yields the frequencies and amplitudes of the cycloidal oscillations in good agreement with the simulation data.

PACS. 75.10.Hk Classical spin models – 05.45.Yv Solitons – 75.40.Mg Numerical simulation studies

1 Introduction

During the past years much attention has been given to the investigation of the structure and dynamics of vortices in magnetic materials of different types [1–17]. These nonlinear topological excitations play an active role in resonance properties of magnets and in the thermodynamics of the Kosterlitz-Thouless vortex-unbinding transition in 2D and quasi-2D magnetic systems (such as magnetic lipid layers, organic intercalated compounds (*e.g.* $(CH)_n(NH_3)_2CuCl_4$) and layered magnets), they are also important for the problem of the Bloch lines in domain walls. Recently the direct experimental visualization of magnetic vortices in magnetic nanodots by magnetic force and Lorentz microscopies measurements [18–20] gave a new impulse to the investigations in this field of the physics of magnetism. Intensive experimental study of artificial 2D lattices of magnetic nanodots in vortex configurations [21] leads to potential applications of these objects in magnetic memory devices. Now even a delicate phenomenon like a shift of the vortex position from the center of a nanodot in an external magnetic field is observed experimentally [20,22]. However, many particular features of vortex dynamics may be studied now only by analytical methods or numerical simulations.

The dynamics of vortices is quite different in ferro- and antiferromagnets and depends essentially on the type and value of the magnetic anisotropy. From the theoretical point of view, the situation in easy-plane ferromagnets with small exchange or single-ion anisotropy seems to be most interesting, because in this case Galilei's law is not valid for a vortex and therefore it exhibits a non-Newtonian dynamics. The structure of this magnetic vortex is in a certain sense similar to that of vortices in a nonideal Bose gas described by Pitaevskii [23] and its dynamics is similar in first approximation to the dynamics of vortices in superfluids. Such a nontrivial dynamics takes place only if the anisotropy is smaller than some critical value and the vortex has a so-called out-of-plane (OP) structure with nonzero components of the magnetization in the hard-axis direction. For this vortex the so-called gyrovector which was defined by Thiele in [1,2] is nonzero and a first-order equation of motion for the vortex center can be derived [3], similar to the Thiele equation for magnetic bubbles and Bloch lines in easy-axis ferromagnets. In an infinite medium without gradients of the magnetization field such an isolated vortex cannot move [5]. A motion is possible only in the presence of a spatial rotation of spins in the easy plane (spin flux) [5]. This is similar to the situation in hydrodynamics, where a vortex in a nondissipative medium can move only with the velocity of the medium, *i.e.* it is "frozen" in the liquid.

In the real situation of a magnet with a finite density of vortices and other magnetic excitations (such as spin waves, for example) and in a confined geometry magnetic vortices can move. In the hydrodynamic approach the interaction with other vortices and the boundaries is simple and leads to vortex motion with average velocity $V \sim 1/\sqrt{n}$, where n is the density of vortices. In a finite ferromagnet with a characteristic size L,

[a] e-mail: franz.mertens@uni-bayreuth.de

a single vortex is subject to Coulomb image forces due to the boundaries; here the above mentioned Thiele equation yields a gyrotropic motion with a small frequency (of order $1/L^2$) [14,15].

But the simulations showed that the real dynamics of an OP-vortex is much more complicated [8–10,14,15]: the motion of two interacting vortices is accompanied by small fast oscillations [8] and even the simple gyrotropic rotation of a single vortex in a finite system is accompanied by an additional cycloidal motion with higher frequencies ($\sim 1/L$) [14,15]. There exist two reasons for this unusual dynamics: the kinematic properties of vortices beyond the hydrodynamic approach and an interaction with spin waves. The characteristic velocities and frequencies of the additional motion of a vortex in the last case are connected with the frequencies and amplitudes of certain spin wave modes (below), which are excited in the system. The excitation of spin waves by a vortex in a nonstationary process and the further interaction with them are interesting from the experimental point of view and may be observed in processes of switching on and switching off an external magnetic field.

In previous articles [9,10,14–16] a new collective variable approach to the nonlinear vortex dynamics was developed for a description of this complicated motion and higher-order generalizations of the Thiele equation were obtained by an improved travelling wave ansatz for the vortex solution. This approach took into account only the own kinematic properties of the vortex (as, for example, its finite mass in the presence of a border or another vortex). In the simple case of the gyrotropic rotation of a vortex in a finite system with size L, the solution of the derived 3rd-order equation of motion gave a good quantitative description of the simulation data for small radii R of rotation ($R \ll L$) [15]. But this agreement was worse for a motion with larger radii R, moreover even for small radius the results for the effective vortex mass from numerical simulation and analytical calculation were different. On the other hand an explanation in terms of interaction with spin waves was not evident as in the simulations all the characteristics of the cycloidal oscillations depended on the parameters L and R in a regular manner while the spin waves due to their linear nature can have arbitrary amplitudes. So the physical origin of the observed oscillations was not clear.

In this article we propose a physical explanation of this phenomenon which gives the possibility to describe with good accuracy all the results observed in the simulations for all values of the parameters R and L. We prove that the interaction with a coherent spin wave is the main reason of the cycloidal oscillations of the vortex.

The main idea of this explanation is the following: at the initial moment when the vortex starts to move it emits a coherent spin wave in order to conserve the total energy and total angular momentum. The amplitude of this coherent wave strongly depends on the initial conditions and in particular on the initial position of the vortex in the system. Later the vortex oscillates in the field of this wave. We investigate analytically such a motion and show that a comparison of the results of our analytical calculations with the simulation data qualitatively confirms this scenario.

In Section 2 we formulate the model and briefly review the main results for the structure of a magnetic OP-vortex. In Section 3 we list and analyse the data from the numerical simulations, and finally in Section 4 we give the theoretical explanation of these data.

2 Model system

Let us consider a classical 2D Heisenberg ferromagnet with easy-plane exchange anisotropy with the Hamiltonian

$$H = -J \sum_{(n,m)} \left(S_n^x S_m^x + S_n^y S_m^y + (1-\delta) S_n^z S_m^z \right), \qquad (1)$$

where J is the coupling constant ($J > 0$ for ferromagnets), δ is the anisotropy parameter ($0 < \delta \leq 1$ for easy-plane symmetry) and the summation is taken over the nearest-neighbor sites of a square-lattice. We treat the spin $\mathbf{S}$ as a classical vector and set later $|\mathbf{S}| = J = 1$.

In the continuum approximation the Hamiltonian (1) can be rewritten as

$$H = \frac{1}{2} \int \mathrm{d}v \Bigg[\left(1 - \delta \left(1 - m^2\right)\right) \frac{(\nabla m)^2}{1-m^2} + \left(1-m^2\right) (\nabla \Phi)^2 + 4\delta m^2 \Bigg], \qquad (2)$$

where $m = S_z$ and $\Phi = \arctan(S_y/S_x)$.

The dynamic equations for this Hamiltonian read [6,24]

$$\frac{\partial \Phi}{\partial t} = m \left[4\delta - (\nabla \Phi)^2\right] - \left[\frac{1}{1-m^2} - \delta\right] \Delta m - \frac{m(\nabla m)^2}{(1-m^2)^2}, \qquad (3)$$

$$\frac{\partial m}{\partial t} = \left(1-m^2\right) \Delta \Phi - 2m \nabla m \nabla \Phi. \qquad (4)$$

The small amplitude solutions of (3, 4) describe linear spin waves with a dispersion relation

$$\omega = ck \left(1 + r_v^2 k^2\right)^{1/2}, \qquad (5)$$

where k is the modulus of the magnon wavevector, c is the magnon velocity and r_v is a characteristic spatial scale ("magnetic length"):

$$c = \sqrt{4\delta}, \quad r_v = \sqrt{\frac{1-\delta}{4\delta}} \simeq \frac{1}{c} \quad \text{for} \quad \delta \ll 1. \qquad (6)$$

In the long-wave approximation ($\partial/\partial r \ll 1/r_v$) the linearized equations (3, 4) reduce to a wave equation for Φ and a connection between the fields Φ and m:

$$\Delta \Phi - \frac{1}{c^2} \frac{\partial^2 \Phi}{\partial t^2} = 0, \qquad (7)$$

$$m = \frac{1}{c^2} \frac{\partial \Phi}{\partial t}. \qquad (8)$$

The simplest nontrivial topological solution of (3, 4) corresponds to a static in-plane (IP) vortex with $m \equiv 0$ and

$$\Phi = q \arctan((y-Y)/(x-X)) \,, \tag{9}$$

where $q = \pm 1, \pm 2, ...$ is a topological charge of the vortex and (X, Y) are the coordinates of its center. But as shown in [6,17] the IP-vortex is stable only if the anisotropy is larger than some critical value δ_c (for the square lattice, $\delta_c \simeq 0.297$). In the domain $\delta < \delta_c$ the IP-vortex is unstable, instead there exists an OP-vortex with a bell-shaped structure of the z-components of the magnetization m. The Φ-field of an OP-vortex in an infinite system has the same form (9) as for the IP-vortex. The spatial distribution of the m-components in the OP-vortex was obtained in [4–6] and has the following asymptotic form near the vortex center and for large distance r from it:

$$m = p\left[1 - a\left(\frac{r}{r_v}\right)^2\right], \; r \to 0, \tag{10}$$

$$m = pb\sqrt{\frac{r_v}{r}}\mathrm{e}^{-r/r_v}, \quad r \gg r_v, \tag{11}$$

where $p = m(r=0) = \pm 1$ characterizes the "polarization" of the vortex; a, b are numerical factors of the order of one, and the above-mentioned magnetic length r_v can be interpreted as the radius of the vortex core. Below we always consider a vortex with $p = q = 1$.

The solution (9–11) is modified when the vortex motion or a finite size of the system is taken into account. For an infinite ferromagnet the deformation of the vortex due to its motion was calculated in [5,6]. For a solution of the form $\mathbf{S} = \mathbf{S}(\mathbf{r} - \mathbf{R})$, where $\mathbf{R} = \mathbf{V}t$ is the position of the vortex center, and for small velocity ($V \ll c$), the deformations in the core are small: $\delta m \sim (V/c)(r/r_v)^3, \delta\Phi \sim (V/c)(r/r_v)$. Outside the core the changes of the azimuthal field are exponentially small ($\delta\Phi \sim \frac{V}{c}(\frac{r_v}{r})^{3/2}\exp(-r/r_v)$) and only the m-components change essentially: it follows from (8) that

$$\delta m \simeq \frac{V}{c}\frac{r_v}{|\mathbf{r}-\mathbf{R}|}|\mathbf{n_r} \times \mathbf{n_v}|, \tag{12}$$

where $\mathbf{n_r}$ and $\mathbf{n_v}$ are the unit vectors in the $(\mathbf{r} - \mathbf{R})$ direction and in the direction of motion, resp.

In a finite system with a vortex situated far from the boundary, the boundary conditions lead first of all to a modification of the Φ-field. The most interesting geometry for us is a circular system (with radius L) and free boundaries (von Neumann boundary conditions); in such a system the solution (9) is modified in the following way

$$\Phi = \arctan\frac{y-Y}{x-X} - \arctan\frac{y-\overline{Y}}{x-\overline{X}} + \arctan\frac{Y}{X}. \tag{13}$$

The second term corresponds to the effective field of an image antivortex at the point $\overline{X} = XL^2/R^2$, $\overline{Y} = YL^2/R^2$ with $R = \sqrt{X^2+Y^2}$. An arbitrary constant can be added to the expression (13), but it is important that the last term in (13) conserves its form for a circular motion of a vortex with $X = R\cos\omega_0 t$, $Y = R\sin\omega_0 t$ ([14]). For a fixed boundary (Dirichlet condition) we must take an image vortex instead of an antivortex and change the sign of the second term in (13).

Using the travelling wave ansatz $\mathbf{S} = \mathbf{S}(\mathbf{r} - \mathbf{R}(t))$ and the Landau-Lifshitz equation

$$\frac{\mathrm{d}\mathbf{S}}{\mathrm{d}t} = -\mathbf{S} \times \frac{\partial H}{\partial \mathbf{S}}, \tag{14}$$

it is easy to derive an effective equation of motion for the vortex center $\mathbf{R}$ (analogous to the Thiele equation) [1,3]:

$$\frac{\mathrm{d}\mathbf{R}}{\mathrm{d}t} \times \mathbf{G} = \mathbf{F}, \tag{15}$$

where the gyrovector $\mathbf{G} = 2\pi pq\mathbf{n}_z$ in our case with positive vorticity and polarization is equal to $2\pi\mathbf{n}_z$ and $\mathbf{F} = -\partial E/\partial\mathbf{R}$ represents an external force acting on the vortex (where E is the energy of the system). In the case of a circular system, $\mathbf{F}$ is the 2D Coulomb force from the image vortex.

In [5] another form of (15) was proposed:

$$\frac{\partial \mathbf{R}}{\partial t} = pq\,(\nabla\Phi_{ex})_{\boldsymbol{r}=\boldsymbol{R}}\,, \tag{16}$$

where Φ_{ex} is a slowly varying external Φ-field at the vortex center. From the solution (13) with the "external" field $\Phi = -\arctan((y-\bar{Y})/(x-\bar{X}))$ and from (16) follow the expressions for velocity V and frequency ω_0 of a pure azimuthal rotation of the vortex

$$V = \frac{R}{L^2 - R^2}, \quad \omega_0 = \frac{1}{L^2 - R^2}. \tag{17}$$

The vortex rotates counter-clockwise (CCW) in the case of free boundary conditions and clockwise (CW) for fixed boundaries.

It follows from (17) that the gyrotropic velocity V of a vortex would diverge at the boundary (for $R \to L$). But a more accurate calculation (see the end of Appendix A) shows that the formula (17) is modified in the narrow vicinity of the boundary and can be approximately rewritten as

$$V \simeq \frac{R}{L^2 - R^2 + r_v L}. \tag{18}$$

This velocity tends to the spin wave velocity c in the limit $R \to L$.

The result (17) can also be obtained from equation (15). It follows from the expression for the energy of a vortex with small velocity and not too close to the boundary ($L - R > r_v$) that (see Appendix A)

$$E = E_0 + \pi \ln\frac{L^2 - R^2}{r_v L}, \tag{19}$$

where the energy of the vortex core $E_0 \simeq 1$.

The analytical results (17) obtained from the Thiele equation are in good agreement with the data of numerical simulation $\omega_0 \simeq 1/L^2$ for small radii R of the gyrotropic rotation. But the first-order equations (15, 16)

can describe only the motion with one frequency – the pure gyrotropic rotation.

That is why in [8,10] a generalized travelling wave ansatz $\mathbf{S} = \mathbf{S}(\mathbf{r} - \mathbf{R}(t), \mathrm{d}\mathbf{R}/\mathrm{d}t)$ was proposed for the description of the complicated vortex motion. But this ansatz is not valid for a finite system. (See, for example, (13).) Therefore we discuss a further modification of the ansatz [9], namely $\mathbf{S}$=$\mathbf{S}(\mathbf{r}, \mathbf{R}(t), \mathrm{d}\mathbf{R}/\mathrm{d}t)$, which leads to the following generalization of equation (15):

$$\hat{\mathbf{M}}\frac{\mathrm{d}^2\mathbf{R}}{\mathrm{d}t^2} + \frac{\mathrm{d}\mathbf{R}}{\mathrm{d}t} \times \mathbf{G} = \mathbf{F}, \tag{20}$$

where the mass tensor $\hat{\mathbf{M}}$ has the components

$$M_{ij} = \int \mathrm{d}v \left(\frac{\partial \Phi}{\partial X_i}\frac{\partial m}{\partial \dot{X}_j} - \frac{\partial \Phi}{\partial \dot{X}_j}\frac{\partial m}{\partial X_i} \right) \tag{21}$$

with $X_i = (X, Y)$ and $\dot{X}_i = (\mathrm{d}X/\mathrm{d}t, \mathrm{d}Y/\mathrm{d}t)$. The mass tensor $\hat{\mathbf{M}}$ is an anisotropic nonlocal complicated characteristic of the vortex and depends strongly on the size and geometry of the system. But for a circular system and small distance of the vortex from its center ($R/L \ll 1$) the tensor $\hat{\mathbf{M}}$ is isotropic ($M_{xx} = M_{yy} = M$) and has the simple form (see Appendix A):

$$M = M_0 + \pi r_v^2 \ln \frac{L}{r_v}, \tag{22}$$

where $M_0 \sim \pi r_v^2$ is the mass of the vortex core.

Although M is a nonlocal quantity, in some sense it plays for a vortex the role of a usual particle mass. For example, the dependences of the field momentum and the energy of the vortex on its velocity in the limit $R/L \ll 1$ have the forms [10]:

$$\mathbf{P} = M\mathbf{V}, \quad E \simeq Mc^2 + \frac{MV^2}{2}\cdot \tag{23}$$

The second order equation (20) permits the existence of more complicated solutions with rapid cycloidal oscillations with the frequency $\omega_c = G/M$, additional to the slow gyrotropic rotation. Such a type of vortex motion was observed in early numerical simulations [8,9], but these cycloidal oscillations had a frequency in the order of $1/L$. So from the above relation it follows that the mass $M = G/\omega_c$ must show a linear dependence on the system size L, in contrast to the predicted logarithmic dependence (22).

Later [14,15], more precise simulations showed a splitting of the frequency of the cycloidal oscillation into a doublet $\omega_{1,2}$ with splitting $\Delta\omega \simeq 4/L^2$ and mean value $\bar{\omega} \simeq 2/(r_v L)$. In order to explain this observation of three different frequencies the generalized ansatz $\mathbf{S} = \mathbf{S}(\mathbf{r}, \mathbf{R}, \mathrm{d}\mathbf{R}/\mathrm{d}t, \mathrm{d}^2\mathbf{R}/\mathrm{d}t^2)$ was made in [15] which yields the 3rd-order equation

$$\hat{\mathbf{A}}\,\frac{\mathrm{d}^3\mathbf{R}}{\mathrm{d}t^3} + \hat{\mathbf{M}}\,\frac{\mathrm{d}^2\mathbf{R}}{\mathrm{d}t^2} - \mathbf{G} \times \frac{\mathrm{d}\mathbf{R}}{\mathrm{d}t} \;=\; \mathbf{F}, \tag{24}$$

with

$$A_{ij} = \int \mathrm{d}v \left(\frac{\partial \Phi}{\partial X_i}\frac{\partial m}{\partial \ddot{X}_j} - \frac{\partial \Phi}{\partial \ddot{X}_j}\frac{\partial m}{\partial X_i} \right). \tag{25}$$

A perturbative solution of the Hamilton equations (3, 4) for free boundary conditions yields a dependence of $m(\mathbf{r})$ on the acceleration of the vortex which was confirmed by computer simulations. For a circular system and small distance of the vortex from its center ($R/L \ll 1$) $\hat{\mathbf{A}}$ is antisymmetric and its only component $A \sim L^2$. The general solution of equation (24) indeed describes the slow gyrotropic rotation of the vortex with the frequency $\omega_0 \sim 1/L^2$ and the high-frequency cycloidal oscillations with the doublet $\omega_{1,2}$ and its mean value $\bar{\omega} \sim 1/L$.

However, the splitting $\Delta\omega \simeq 2\ln(L/r_v)/L^2$ is larger than the value $4/L^2$ from the simulations. More importantly, as $\Delta\omega \sim M/A$ from equation (24), this would imply a constant mass in contrast to the logarithmic L-dependence in equation (22). For increasing R/L the discrepancies become larger, and for $R/L \to 1$ the vortex mass, calculated from (24) using our new simulation data, would even become negative.

Apart from these discrepancies, the phenomenological equation (24) does not provide a *physical* explanation for the cycloidal oscillations. Such an explanation is the aim of our paper.

3 Computer simulations of the vortex motion

To answer the above questions we first list and discuss in detail the results of numerical simulations of the vortex motion, which extend earlier simulations [15].

The simulation studies were performed on a square lattice for a circular system with free boundary conditions using the discrete analogue of equations (3, 4) with $\delta = 0.1$ (in this case $r_v = 1.5$ and $c = 0.63$). These calculations were carried out for several sizes of the circle ($L = 24, 36, 72$) and different initial positions of the vortex center ($R = 4, 6, 8, 10, 12, 14, 16$ for $L = 24$; $R = 6, 8, 10, 12, 16, 20, 24, 28$ for $L = 36$ and $R = 8$, 16, 24, 32, 40, 48, 56 for $L = 72$). The data from the simulations are presented in Table 1, which also contains the earlier data for $R/L < 0.3$ from [15].

As the exact structure of the vortex is not known analytically even for an infinite system, in a first stage of the simulation a static solution of the Landau-Lifshitz equations (3, 4) is found by an iteration procedure for the vortex situated in the center of the system under consideration (for details see [15]). Then this static solution is shifted from the center of the circle to a position at the distance R from it.

In a second stage of the simulation (for time $t > 0$) the dynamical terms of the Landau-Lifshitz equations are taken into account, and the vortex starts to move in the CCW-direction. A typical trajectory of the vortex was presented in [16] (Fig. 4) for the system with radius $L = 36$ and starting coordinate $R(0) = 12$.

It is evident from the results of the simulation that the motion of a single vortex with polar coordinates $R = \sqrt{X^2 + Y^2}$ and $\chi = \arctan(Y/X)$ is a superposition of a constant rotation along a circle $R = R_0$, $\chi = \omega_0 t$ with gyrotropic frequency ω_0 and additional oscillations

Table 1. Simulation data for the vortex motion on a circle of radius L. R_0 and ω_0: radius and frequency of the gyrotropic rotation; ω_1 and ω_2: doublet of cycloidal oscillations; $\overline{\omega}$ and Ω: mean frequency and splitting of the doublet; a_i and b_i: radial and azimuthal amplitudes of the oscillations.

L	R_0	ω_0	ω_1	ω_2	$\overline{\omega}$	Ω	a_1	a_2	b_1	b_2
24	4.026	0.00184	0.04441	0.05120	0.04781	0.00339	0.08978	0.08457	0.09067	0.08954
24	6.021	0.00190	0.04447	0.05088	0.04767	0.00321	0.13713	0.12360	0.14161	0.13746
24	8.019	0.00301	0.04463	0.05049	0.04756	0.00293	0.17303	0.15186	0.18347	0.17973
24	10.064	0.00316	0.04482	0.05006	0.04744	0.00262	0.20204	0.17228	0.22211	0.21999
24	11.953	0.00237	0.04500	0.04963	0.04730	0.00231	0.21600	0.18440	0.24321	0.25436
24	13.967	0.00269	0.04525	0.04920	0.04722	0.00197	0.23212	0.17432	0.28157	0.27445
24	15.908	0.00317	0.04551	0.04876	0.04713	0.00163	0.23320	0.16789	0.31211	0.29812
36	5.802	0.000814	0.03039	0.03347	0.03193	0.00154	0.0754	0.0896	0.0754	0.0911
36	8.278	0.000823	0.03044	0.03335	0.03189	0.00145	0.143	0.116	0.0147	0.126
36	9.870	0.000852	0.03049	0.03327	0.03188	0.00139	0.144	0.130	0.152	0.146
36	12.250	0.000888	0.03055	0.03315	0.03185	0.00130	0.185	0.163	0.195	0.186
36	16.016	0.000982	0.03067	0.03293	0.03179	0.00113	0.212	0.176	0.242	0.232
36	19.980	0.001114	0.03084	0.03266	0.03175	0.00091	0.225	0.186	0.276	0.280
36	23.911	0.001414	0.03101	0.03242	0.03171	0.00071	0.225	0.170	0.318	0.316
36	27.890	0.001971	0.03122	0.03219	0.03170	0.00048	0.197	0.142	0.340	0.326
72	8	0.000201	0.01566	0.01642	0.01604	0.00038	0.0656	0.0638	0.0594	0.0602
72	16.1	0.000205	0.01566	0.01641	0.01603	0.00037	0.1224	0.1250	0.1160	0.1273
72	24.2	0.000218	0.01569	0.01635	0.01602	0.00033	0.1681	0.1591	0.1887	0.1936
72	31.9	0.000243	0.01574	0.01628	0.01601	0.00027	0.1989	0.1721	0.2460	0.2364
72	40	0.000282	0.01580	0.01622	0.01601	0.00021	0.2081	0.1837	0.2877	0.2877
72	48	0.000350	0.01584	0.01616	0.01600	0.00016	0.2015	0.1675	0.3262	0.3310
72	55.9	0.000492	0.01591	0.01611	0.01601	0.00010	0.1812	0.1486	0.3242	0.3242

with higher frequency. As one can see from Table 1 the average radius R_0 of the gyrotropic motion slightly differs from the initial radius. In [15] the dependence of the vortex position on the time was discussed in detail and for the initial radius $R(0) = 12$ the trajectory $R(\chi)$ was plotted in a large scale in Figure 4. The radial displacement $\tilde{r}(t) = R(t) - R_0$ from the mean trajectory is in the order of 0.3. The corresponding Fourier spectrum of $\tilde{r}(t)$ was shown in [15] in Figure 5. (Note that this spectrum was evaluated in a rotating coordinate frame and so it does not contain a peak at $\omega_0 = 0.00089$ corresponding to the gyrotropic rotation.) This spectrum clearly shows two dominant frequencies $\tilde{\omega}_1 = 0.02966$ and $\tilde{\omega}_2 = 0.03404$ with approximately the same amplitude, (a small additional peak at $4\omega_0$ appears due to the nonhomogeneous boundary condition on the circle boundary for a square lattice.) The Fourier spectra have such a simple structure in a wide interval of values of R/L, but for $R/L \to 1$ where the trajectories are close to the boundary of the circle, this structure becomes more complicated: a lot of additional peaks appear with amplitudes in the order of the dominant peaks and the amplitudes of these peaks become different.

It is important to analyse the time evolution of the spatial distribution of the magnetization m to understand in detail the spin dynamics of the system. Typical distributions of the z-components of the spins for the case $L = 36, R = 12$ were shown in Figures 1 and 2 of [15]. These figures demonstrate that the vortex moves on the background of a spin wave and the radial coordinate R in Figure 4 [15] oscillates in phase with the change of polarity of the spin wave.

Now in Figure 1 we show the distribution of magnetization at the initial stage of motion for $t = T_0/360$ ($T_0 = 2\pi/\omega_0$ represents the period of the gyrotropic rotation). We see that at this moment, when the vortex starts to rotate in the CCW-direction from the position $X = -R, Y = 0$, a standing coherent spin wave is formed with maxima of the m-field of order of 0.025 at the points $x = 0, y = \pm L$. Later this wave oscillates with the high frequency $\overline{\omega} \simeq 0.032$ and slowly rotates in the opposite CW-direction with the frequency $\Omega \simeq 0.0013$. (During the time interval $\Delta t = T_0/6$ the vortex rotates by the angle $\Delta\chi = \pi/3$ and the standing wave rotates by the angle $-\pi/2$. In this period the maximum amplitudes of the spin wave are in the order of 0.03.) Comparison of these data with the spectrum in Figure 5 of [15] shows that $\overline{\omega} \simeq (\tilde{\omega}_1 + \tilde{\omega}_2)/2$ and $\Omega \simeq [(\tilde{\omega}_2 - \omega_0) - (\tilde{\omega}_1 + \omega_0)]/2$. So the excited coherent spin wave is a superposition of two modes: The first mode rotates in the CCW-direction with frequency $\omega_1 = \tilde{\omega}_1 + \omega_0$ in the laboratory frame and corresponds to the low-frequency peak in Figure 5 [15] and the second mode rotates in the CW-direction with $\omega_2 = \tilde{\omega}_2 - \omega_0$ and corresponds to the higher-frequency

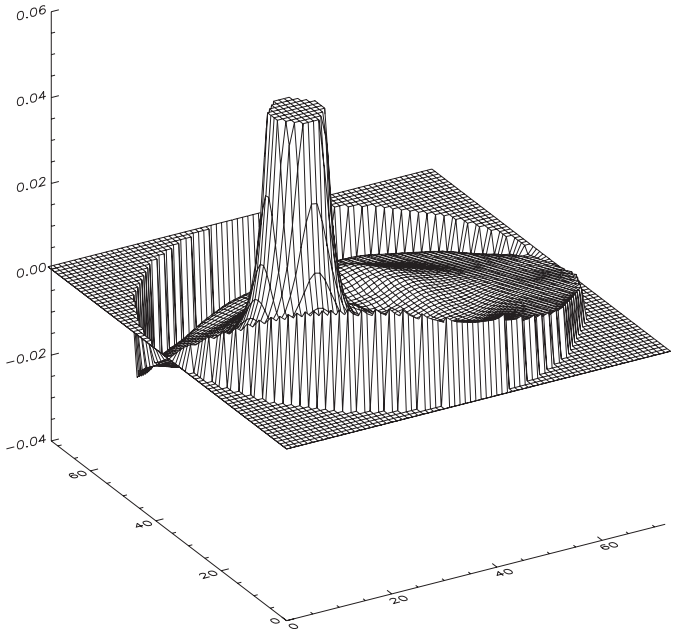

Fig. 1. Distribution of the m-components of the magnetization for a circular system with radius $L = 36$ with a vortex at distance $R = 12$ from the center at the time $t_0 = T_0/360$ immediately after the beginning of the motion.

peak. In the laboratory frame these dominant peaks have the frequencies $\omega_1 = 0.0305$, $\omega_2 = 0.0332$.

In order to prove that the dominant frequencies of the spectrum indeed correspond to spin waves, we took into account a small damping in the Landau-Lifshitz equations (14) and checked that the amplitudes of these main peaks decrease exponentially in time and the decrement of their damping exactly agrees with the decrement of linear spin waves.

The excited coherent standing spin wave can be represented approximately as

$$m \simeq f(r)\,(B_1 \cos(\varphi - \omega_1 t) + B_2 \cos(\varphi + \omega_2 t)) \qquad (26)$$

where $r = \sqrt{x^2 + y^2}$ and $\varphi = \arctan(y/x)$ are polar coordinates in space, $B_1 \simeq B_2$ and $\omega_1,\ \omega_2 > 0$. In reality, in the presence of a vortex the structure of these modes is more complicated. In [7,11–14,16,25] the normal modes of finite easy-plane ferromagnets with a vortex situated in the center of the system were studied in detail for circular and square systems, for different sizes and both Dirichlet and von Neumann conditions.

The typical structure of the spectrum of these eigenmodes and its dependence on the anisotropy parameter δ is shown in Figure 2, taken and enlarged from [11]. These dependencies are depicted only for three lower modes which are most interesting for us, namely the modes with unit azimuthal number, *i.e.* with the form $m \sim \cos(\pm\varphi - \omega t)$. We see that at the critical value $\delta_c \simeq 0.297$ (where the OP-vortex structure appears) these eigenfrequencies split into the doublets $(aa'), (bb'), (cc')...$ The upper branches of these doublets $(a, b, c...)$ have the positive azimuthal number and the corresponding modes rotate in the CCW-direction, the lower branches $(b', c'...)$

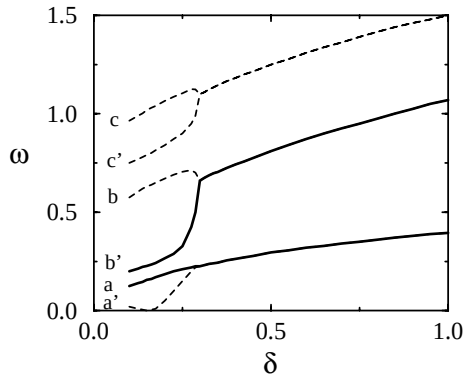

Fig. 2. The frequencies of the lowest azimuthal modes as a function of the anisotropy parameter δ for a circular system with radius $L = 7.5$ and free boundary conditions in the presence of a vortex in the center of the system (from [11]). The modes (a, b') correspond to the main doublet in the Fourier spectrum in Figure 5 of [15].

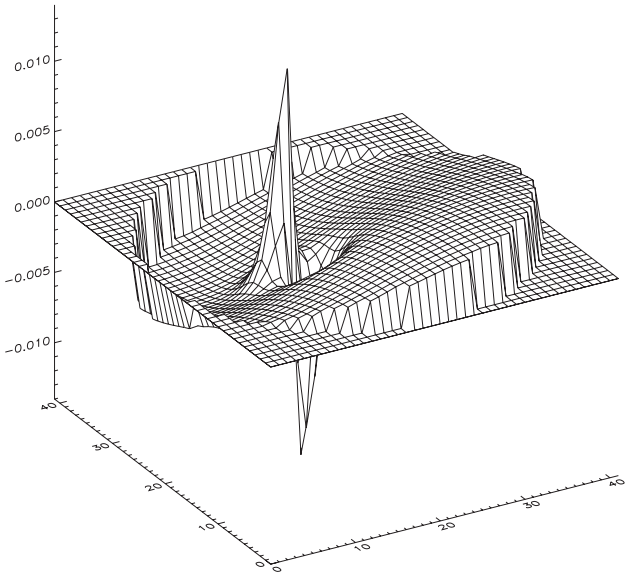

Fig. 3. The profile of the azimuthal mode corresponding to the a-branch of the spectrum in Figure 2.

with the negative azimuthal number correspond to modes rotating in the CW-direction (with the exception of the a'-mode which rotates in CCW-direction). The dominant modes excited in the numerical simulations correspond to the upper branch of the first doublet and the lower branch of the second doublet (branch a has the frequency ω_1 and branch b' has the frequency ω_2). The superposition of the a and b' branches rotates in the CW-direction because $\omega_2 > \omega_1$.

Outside the core of the vortex the eigenmodes of the upper branches of the doublets differ only slightly from the corresponding eigenmodes of a system without a vortex. (See Fig. 3 where the profile of the a-mode is represented for a circular domain with radius $R = 20$ and free boundaries.)

The eigenmodes of the lower branches of the doublets differ strongly from the corresponding modes in the absence of the vortex. But in the limit of small anisotropy

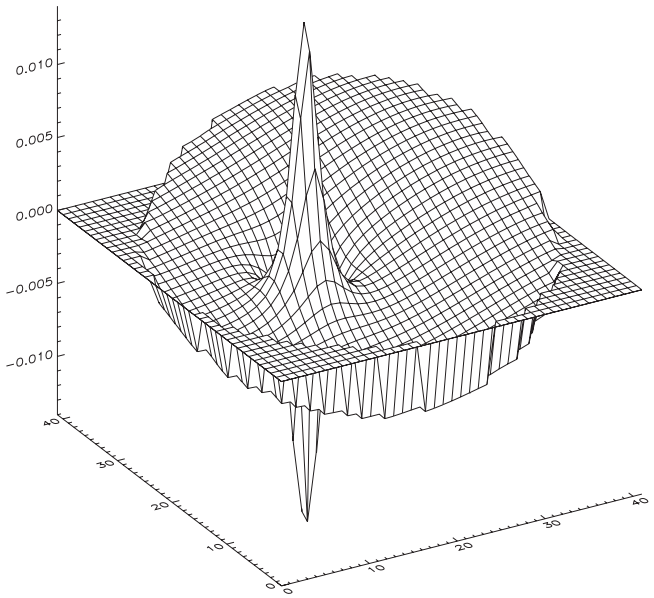

Fig. 4. The same as in Figure 3 but for the b'-branch.

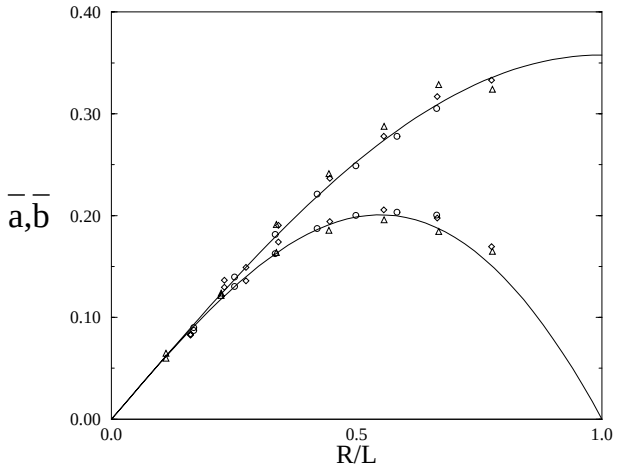

Fig. 5. The mean amplitudes $\overline{a}, \overline{b}$ of the radial and azimuthal oscillations (lower and upper branch, resp.) as functions of R/L. The numerical results for $L = 24$ (□), 36 (◊) and 72 (△) in comparison with analytical results (solid lines), reduced by a factor of 1.03.

($\delta \ll 1$) they change in such a way that in all the area outside the vortex core the profiles of these modes become similar to those for the upper branch of the previous doublet. (Compare the forms of the b'-mode (Fig. 4) and the a-mode (Fig. 3).) So outside the vortex core the distribution of the magnetization in the dominant modes is similar to the ground mode with unit azimuthal number in the same system without a vortex.

It was shown in [15] that the simulation data for the time dependencies of the radial displacement $\tilde{r}(t) = R(t) - R_0$ and the azimuthal displacement in the rotating frame $R_0\tilde{\chi}(t) = R_0(\chi - \omega_0 t)$, are described very accurately by the ansatz

$$\tilde{r}(t) \;=\; a_1 \;\cos\tilde{\omega}_1 t \;+\; a_2 \;\cos\tilde{\omega}_2 t\,, \qquad (27)$$

$$R_0\;\tilde{\chi}(t) \;=\; b_1 \;\sin\tilde{\omega}_1 t \;-\; b_2 \;\sin\tilde{\omega}_2 t, \qquad (28)$$

where $a_i, b_i > 0$.

For $R_0/L < 0.2$ the amplitudes of the two modes with the frequencies $\tilde{\omega}_1$ and $\tilde{\omega}_2$ are approximately equal ($a_1 \simeq a_2,\ b_1 \simeq b_2$) and for this case

$$\tilde{r}(t) \simeq 2a\ \cos\overline{\omega}t\ \cos\tilde{\Omega}t\,,\quad R_0\tilde{\chi}(t) \simeq 2b\ \cos\overline{\omega}t\ \sin\tilde{\Omega}t, \qquad (29)$$

where $\tilde{\Omega} = (\tilde{\omega}_2 - \tilde{\omega}_1)/2$ and $\overline{\omega} = (\tilde{\omega}_2 + \tilde{\omega}_1)/2$. (Note that the total amplitude of these oscillations is of order of $2a$.)

So in the moving frame of reference the center of the vortex oscillates with the frequency $\overline{\omega}$ and the polarization of these oscillations rotates with the small frequency $\tilde{\Omega}$. This character of the oscillations is evident from Figure 4 from [15].

Table 1 contains for different values of L and R_0 the observed values for the frequency ω_0 of the gyrotropic rotation, the dominant frequencies ω_1 and ω_2, their mean frequency $\overline{\omega}$, the splitting Ω of the frequencies (all in laboratory frame) and the amplitudes a_i and b_i of the oscillations.

This table shows a good agreement between the data for ω_0 and the formula (17). The mean frequency $\overline{\omega}$ of the two dominant modes depends very slightly on R_0 and agrees with good accuracy with the analytical result for the ground rotating eigenmode in a circular system without a vortex. The solution of equations (7, 8) for this mode is well known:

$$m \;=\; m_{max}\;\frac{J_1\,(r\omega/c)}{J_1\,(z_1)}\;\sin(\varphi - \omega t), \qquad (30)$$

where m_{max} is the amplitude of the wave, $J_1(\rho)$ is a Bessel function and for free boundary conditions $\mathrm{d}J_1(\rho)/\mathrm{d}\rho|_{\rho=z_1} = 0$ where $z_1 \simeq 1.8412$. The eigenfrequency of this mode is $\omega = (cz_1/L)$. For $L = 24, 36, 72$ we have a set of frequencies $\omega = 0.0485;\ 0.0323;\ 0.0162$ very close to the data for $\overline{\omega}$ in Table 1.

The frequency Ω of the slow rotation of the excited stationary wave depends strongly on the ratio R/L and the system size L. For small radii there is a good agreement with the analytical result obtained in [16]:

$$\Omega(R \to 0) \;\simeq\; \frac{\pi}{4L^2}\frac{z_1 Y_1'(z_1)}{J_1''(z_1)} \;\simeq\; \frac{2}{L^2}, \qquad (31)$$

where Y is a Neumann function.

But in the region $R/L > 0.2$ the analytical formula (31) and the data from the simulation disagree: Ω decreases with increasing R/L and can be approximated by the formula $\Omega \simeq 2.6(1 - R/L)/L^2$.

Table 1 shows that the amplitudes of the cycloidal oscillations are small (m_{max} for $L = 36,\ R = 12$ is of order of 0.3) and grow with the radius of the gyrotropic rotation. The amplitudes b_1 and b_2 of the azimuthal oscillations are equal with good accuracy for all $0 < R < L$. The difference between the amplitudes a_1 and a_2 of the radial oscillations grows with the ratio R/L: $(a_1 - a_2)/a_1 \simeq (R/L)/\ln(L/r_v)$.

The mean amplitude $\overline{b} = (b_1 + b_2)/2$ of the azimuthal oscillations grows linearly with R/L in a wide interval, only for $R/L > 0.5$ the increase becomes smaller (see upper branch in Fig. 5). The mean amplitude $\overline{a}$ of the radial

oscillations grows linearly for small R/L, at $R/L \simeq 0.55$ a maximum is seen (lower branch in Fig. 5).

4 Theoretical description of the cycloidal vortex motion

For an explanation of the main features of the complicated vortex dynamics we propose the following simple scenario:

When the vortex is shifted from the center of the circle to the position with R at $t = 0$, the magnetization distribution in the system does not agree with the equilibrium distribution of a static vortex with the center at R. It follows from equation (19) that in this case the vortex has the extra potential energy $\delta E = -\pi \ln(1 - R^2/L^2)/2$ which is about 0.185 for $L = 36$ and $R = 12$. (The total vortex energy is in the order of 10 in this case). At the moment $t = 0$ from which the dynamical Landau-Lifshitz equations are solved, the vortex starts to move and the magnetization distribution in it adapts to the solution of these equations. For $t > 0$ the motion of the vortex mainly consists of a gyrotropic rotation with average radius R_0, velocity V and frequency ω_0 given by formula (17). The structure of the moving vortex is slightly modified proportionally to the small velocity V, as follows from equation (12), and it appears a small total magnetization of the vortex in the order of $\pi r_v^2 RV (\simeq 0.75$ for $R = 12, L = 36)$. But the additional kinetic energy of the gyrotropic motion is very small: for our parameters it is in the order of 0.001 (so the kinematic effects are small, too). Thus the main part of the extra vortex energy is emitted into the volume as a spin wave. This process is much quicker than the vortex motion. The excited spin wave reaches the boundary of the system after the time interval $\delta t \simeq cL \simeq 22$ (close to the time $t_0 = T_0/360$ corresponding to Fig. 1) and forms the coherent eigenmode shown in this figure.

From the comparison of (9) and (13) it is evident that the discrepancy between the initial (9) and equilibrium (13) distributions of the magnetization for small radii $R \ll L$ has the form $\Delta\Phi \simeq -(R/L^2) r \sin\varphi$, *i.e.* the form of the first azimuthal mode of the spin waves (*cf.* (30)). But from Figures 3, 4 we see that in the presence of a vortex *two* internal modes of the system have such a symmetry. So to fulfil the boundary conditions the extra energy of the vortex must transform into the energy of this spin wave doublet. As the frequency of the gyrotropic motion is extremely small ($\omega_0 \simeq 1/L^2$) only the lowest eigenmodes of the spin system can be effectively excited.

The rotating vortex has an additional angular momentum in comparison with the static vortex at the same distance from the center. But the total angular momentum of the system is an integral of motion. Thus the additional momentum of the moving vortex must be compensated by a shift of the radius of the gyrotropic rotation (which we see in Fig. 4 of [15]) and by the angular momentum of the excited spin waves. As the average radial position R_0 of the vortex grows very slowly the angular momentum of the spin waves in the direction opposite to the vortex rotation must arise during the initial stage of the process. The lowest eigenmode has radial symmetry and zero angular momentum and so the next higher modes with unit azimuthal number must be excited (this is in an agreement with the above estimation of the exited field). For small δ the lowest azimuthal mode (a' in Fig. 2) transforms into the CCW rotation of the vortex.

Therefore this wave cannot compensate the angular momentum of the vortex. The azimuthal mode rotating in the CW-direction (mode b' in Fig. 2) has a momentum opposite to the azimuthal vortex momentum and can in principle compensate it. But the average angular momentum of the vortex in the situation under consideration is of order of 2.7 (see the calculation below) while the momentum of the b'-mode is smaller by a factor of two. Moreover, as we see from the simulation that a coherent superposition of two spin waves (29) arises, with the same amplitudes and a total angular momentum of order of 0.5. The superposition of the principal azimuthal modes (a and b') rotates in CW-direction because $\omega_2 > \omega_1$, and compensates a part of the total angular momentum of the vortex. We see this slow CW-rotation of the coherent spin wave in our simulations.

The excited wave rotates independently from the vortex in the first approximation and we can neglect an influence of the vortex on its dynamics. But the influence of these eigenmodes on the vortex leads to oscillations of its center in the periodical time-dependent field of the spin wave.

We cannot solve analytically the initial value problem for the beginning of the vortex motion and the excitation of coherent modes. So we shall use the conservation laws of the system under consideration. Unfortunately there exist only three such integrals of motion: total z-component of the magnetization, total angular momentum and energy, while the solution for the excited system depends on a much larger number of parameters such as the amplitudes of the excited eigenmodes, the shift of the average vortex orbit, the background of magnetization and so on. That is why we use the results of our analysis of the numerical simulations and assume that only two dominant low-frequency CW- and CCW-modes with unit azimuthal numbers and approximately equal amplitudes are excited in the system.

First of all we must calculate the initial energy of the vortex and the energies of the two excited spin waves. A vortex situated in the center of the circle has a simple configuration with $\Phi = \arctan(y/x)$, and its energy from (19) is $\pi \ln(L/r_v)$. At the moment $t = 0$ the vortex was shifted by the distance R from the center, *i.e.* the field distribution has the form $\Phi = \arctan((y + R)/x)$. It is easy to show that the energy of this configuration $E = \pi \ln(L/r_v) + \pi/2 \ln(1 - R^2/L^2)$ is larger than the energy of the equilibrium static vortex (19) by the amount

$$\delta E_V = -\frac{\pi}{2} \ln\left(1 - \frac{R^2}{L^2}\right). \tag{32}$$

As the z-component of the magnetization field in the static vortex decreases exponentially with the distance

from its center, the total $z-$component of the vortex due to its core is of order of $\mu = \pi r_v^2$ and the background field is absent: $m_0 = 0$.

The angular momentum of a static vortex follows from (59)

$$K_V \;=\; \pi(L^2 - R^2), \tag{33}$$

and strongly depends on its position on the circle.

At the moment $t = 0$ when the vortex starts to move its simple initial configuration of the magnetization relaxes to the rotating vortex solution (13) with $\chi = \omega_0 t$ and nonzero m-field: $m \simeq \dot{\Phi}/c^2$. As follows from (57, 62) the kinetic energy of a moving vortex $E_c \simeq \pi r_v^2 R^2/2L^4(\ln(L/r_v) + 5/4)$ is extremely small ($E_c \sim 0.001$ for $L = 36$ and $R = 12$). So all the extra energy δE_V (~ 0.185 for$L = 36, R = 12$) transforms into the energy of spin waves.

In the moving vortex a nonzero magnetization appears additionally to the one of the vortex core. From (60) the total additional z-component is $\Delta\mu \simeq \pi r_v^2 R^2/(L^2 - R^2)$. As μ is an integral of motion a uniform background with

$$m_0 = \frac{r_v^2 R^2}{L^2(L^2 - R^2)} \tag{34}$$

($\simeq 0.0002$) must be excited in the system. (The corresponding frequency of a uniform spin rotation is very small: $\simeq 0.0001$.)

The total angular momentum of the vortex moving with average radius R_0 on this background is (see (64))

$$K_V = R_0 V \pi r_v^2 \left(\ln\frac{L}{r_v} + \frac{\varepsilon^2 + 2\varepsilon - 1}{2\varepsilon^2}\ln(1-\varepsilon) - \frac{1}{2\varepsilon} + 1 - \varepsilon \right) + \pi\left(L^2 - R_0^2\right), \tag{35}$$

where $\varepsilon = R_0^2/L^2$. We took into account that the position of the vortex can shift and the radius R_0 of the gyrotropic rotation can differ from the initial radius R.

For not very large radius of rotation the change in vortex angular momentum is

$$\delta K_V = \pi r_v^2 \frac{R_0^2}{L^2}\left(\ln\left(\frac{L}{r_v}\right) + \frac{1}{4}\right) - \pi\left(R_0^2 - R^2\right). \tag{36}$$

The first term in (36) is approximately equal to 3 for $L = 36, R = 12$. So the shift of the radius considerably changes the angular momentum.

Now let us calculate the integrals of motion for the excited principal modes. In the absence of the vortex the superposition of these CW- and CCW-modes in a circular sample with free boundaries has the form:

$$\Phi_{sw}(\mathbf{r}, t) = A_1 J_1\left(\frac{r\omega}{c}\right)\sin(-\varphi + \omega t) + A_2 J_1\left(\frac{r\omega}{c}\right)\sin(\varphi + \omega t), \tag{37}$$

with the same frequency $\omega = \overline{\omega} = cz_1/L$.

As was shown in [16] in the presence of a vortex situated in the center of a circle the solution (37) is modified outside of the vortex core in the following manner:

$$\Phi_{sw}(\mathbf{r}, t) = A_2\left(J_1\left(\frac{r\omega_2}{c}\right) + \frac{\pi}{4}\frac{r_v\omega_2}{c}\,Y_1\left(\frac{r\omega_2}{c}\right)\right) \times \sin(\varphi + \omega_2 t) + A_1\left(J_1\left(\frac{r\omega_1}{c}\right) - \frac{\pi}{4}\frac{r_v\omega_1}{c}\,Y_1\left(\frac{r\omega_1}{c}\right)\right) \times \sin(-\varphi + \omega_1 t), \tag{38}$$

where $\omega_1 = \overline{\omega} - \Omega \simeq \overline{\omega} - 2/L^2$ and $\omega_2 = \overline{\omega} + \Omega \simeq \overline{\omega} + 2/L^2$.

From equations (37, 38) it is evident that the total magnetization μ of the spin waves is zero and we must calculate only their energy and angular momentum. In the first approximation we shall neglect the small additional terms with Neumann functions Y_1 in (38) which are proportional to the small values $\omega_{1,2} \sim 1/L \ll 1$ and result from the existence of the vortex in the system. Nevertheless we take into account that in the presence of the vortex the frequencies ω_1 and ω_2 in the arguments of the Bessel functions and in the trigonometric functions are not equal and depend on the rotation radius R_0. We use the relation $J_1(r\omega_{1,2}/c) \simeq J_1(\rho) \mp (r\Omega/c)\ \mathrm{d}J_1(\rho)/\mathrm{d}\rho$ with $\rho = r\overline{\omega}/c$, take into account the relation (8) for small amplitude spin waves and obtain the energy of each principal mode in (38)

$$E_{sw}^i = \frac{\pi}{2}A_i^2(z_1^2 - 1)J_1^2(z_1) \simeq 1.27A_i^2. \tag{39}$$

In this approximation the angular momentum (58) of each rotating spin wave in (38) can be reduced to the form

$$K_{sw}^i \;=\; -\,\frac{\omega_i}{c^2}\int \mathrm{d}v\left(\frac{\partial\Phi_{sw}^i}{\partial\varphi}\right)^2. \tag{40}$$

Substitution of the solution (38) into this formula gives

$$K_{sw}^{1,2} \simeq A_{1,2}^2\pi r_v^2\left(\pm\,\beta\,\frac{L}{r_v} \;-\alpha\,(\Omega L^2)\right) + \mathcal{O}(\Omega^2) \simeq A_{1,2}^2\left(\pm 0.6L - 3.5\right), \tag{41}$$

where $\alpha = J_1^2(z_1)(z_1^2+1)/2z_1^2 \simeq 0.22$ and $\beta = J_1^2(z_1)(z_1^2-1)/2z_1^2 \simeq 0.12$. (We took into account that $\Omega L^2 \simeq 2$ for small R_0/L as was shown in [16].)

As it follows from the numerical data the amplitudes of the principal modes are closely allied $A_1 \simeq A_2 = A$ and so the sum of their energies is $E_{sw} \simeq 2.54A^2$. This must be equal to the extra energy of the starting vortex (32). This comparison gives us the dependence of the amplitudes of the excited coherent spin waves on the radius of gyrotropic rotation and the size of the system:

$$A \;=\; \frac{R_0}{L}\;\frac{1}{J_1(z_1)\sqrt{2(z_1^2-1)}} \;\simeq\; 0.786\frac{R_0}{L}. \tag{42}$$

The amplitude of the Φ- field in the coherent spin wave is equal to $\Phi_{max} = 2AJ_1(z_1) \simeq 1.16A \simeq 0.91R_0/L$ and this result is in good agreement with the above estimate for $\Delta\Phi_{max} \simeq (rR_0/L^2)|_{r=R_0}$. The amplitude of

the m-field is $m_{max} = 2AJ_1(z_1)z_1/cL \simeq 3.4A/L$. For $R = 12, L = 36$ we have $A \simeq 0.262$, $\Phi_{max} \simeq 0.3$, and $m_{max} \simeq 0.025$, and the last result agrees with good accuracy with the value observed in the simulations (see Fig. 1.)

In the above simple approach it is easy to calculate the total angular momentum of the superposition of stationary coherent spin waves (see Appendix B). In the first approximation in the small parameter $1/L \ll 1$ the angular momentum has the form

$$K_{sw} = -A^2 \ 2\pi r_v^2 \ (\alpha \Omega L^2 \ - \beta \ \frac{L}{r_v} \frac{A_1 - A_2}{A} - \beta \ \cos 2\overline{\omega} t). \quad (43)$$

We see that due to the interference of the principal modes the angular momentum K_{sw} oscillates in time and therefore such a superposition of spin waves can exist only in the presence of another excitation with oscillating angular momentum (in our case an oscillating vortex).

It follows from the numerical data (see Tab. 1) that the difference in the amplitudes of the principal modes grows with the ratio R_0/L and slightly depends on the system size L: $(A_1 - A_2)/A_1 \simeq (R_0/L)/\ln(L/r_v)$. The average value of the angular momentum of the coherent spin waves for small distance of the vortex from the center (when $\Omega L^2 \simeq 2$) is

$$\overline{K}_{sw}(R_0 \ll L) \ \simeq - \ A^2 \ \left(7 - 1.2 \ \frac{R_0}{\ln(L/r_v)}\right). \quad (44)$$

For $L = 36, R = 12$ using (42) we have $\overline{K}_{sw} \simeq -0.165$. So the total angular momentum of the principal modes is much smaller than the first term in (36) for the change of the vortex momentum. Then it follows from the condition $\delta K = 0$ and from the formulae (36) that the shift of the vortex radius of motion must be in the order of

$$\frac{\Delta R}{R_0} \simeq \frac{r_v^2}{2L^2} \left(\ln \frac{L}{r_v} + \frac{1}{4}\right). \quad (45)$$

Unfortunately the spread of the numerical data for this quantity is rather large (see Tab. 1) and it even changes its sign. But the average value of $\Delta R/R_0 \sim 10^{-2}$ has the same order as in equation (45).

The final expression for the excited principal modes in the first approximation has the following simple form

$$\Phi_{sw}(\mathbf{r}, t) \simeq \frac{R_0}{L} \ \frac{1}{z_1\sqrt{\beta}} \ J_1\left(\frac{r}{L} z_1\right) \sin \overline{\omega} t \ \ \cos(\varphi + \Omega t), \quad (46)$$

$$m_{sw}(\mathbf{r}, t) \simeq \frac{R_0}{cL^2} \ \frac{1}{\sqrt{\beta}} \ J_1\left(\frac{r}{L} z_1\right) \cos \overline{\omega} t \ \ \cos(\varphi + \Omega t). \quad (47)$$

These expressions give the dependencies of the characteristics of the coherent spin wave on the parameters R_0 and L.

At last we must use these dependencies and find the relation between the amplitude of these excited modes and the amplitude of the cycloidal secondary vortex motion in the spin wave field. To do this we use equation (16), insert the solution (46) and take into account the field of the antivortex. In our simplest approximation the "external" Φ-field has the form

$$\Phi_{ex} \simeq \frac{R_0}{L} \ \frac{1}{z_1\sqrt{\beta}} \ J_1\left(\frac{R_0}{L} z_1\right) \sin \overline{\omega} t \ \ \cos(\chi + \Omega t) + \Phi_{AV}(r = R_0, \varphi = \chi), \quad (48)$$

where the last term $\Phi_{AV} = -\arctan((y - \overline{Y})/(x - \overline{X}))$ corresponds to the field of the image antivortex. Substituting this function into (16) we rewrite the system of equations for the cycloidal vortex oscillations

$$\frac{\mathrm{d}R}{\mathrm{d}t} \simeq \frac{R}{L^2} \frac{1}{\sqrt{\beta}} \left(\frac{\mathrm{d}J_1(\rho)}{\mathrm{d}\rho}\right)_{r=R} \sin \overline{\omega} t \ \cos(\chi + \Omega t), \quad (49)$$

$$R \ \frac{\mathrm{d}\chi}{\mathrm{d}t} \simeq - \ \frac{1}{L} \frac{1}{z_1\sqrt{\beta}} \ J_1(\rho)|_{r=R} \sin \overline{\omega} t \ \sin(\chi + \Omega t) \ + \ \omega_0 R, \quad (50)$$

where R and χ are the polar coordinates of the vortex and $\rho = r z_1/L$. This is a complicated system of nonlinear time-dependent equations. But for the vortex oscillating with a small amplitude we can put

$$R = \overline{R} + a_r, \quad \chi = \omega_0 t + a_\chi/\overline{R}\,, \quad (51)$$

where $a_r, \ a_\chi \ll \overline{R}$, and replace χ by $\omega_0 t$ and R by $\overline{R}$ on the righthand sides of this system, (the new veriables a_r and a_χ correspond to $\tilde{r}(t)$ and $R_0\tilde{\chi}(t)$ in the phenomenological formula (29)). Then equations (49, 50) can be trivially integrated and the result has the simple form

$$a_r \simeq \frac{1}{z_1 c\sqrt{\beta}} \frac{\overline{R}}{L} \left(\frac{\mathrm{d}J_1(\zeta)}{\mathrm{d}\zeta}\right) \cos \overline{\omega} t \ \cos \tilde{\Omega} t \ , \quad (52)$$

$$a_\chi \simeq \frac{1}{z_1^2 c\sqrt{\beta}} J_1(\zeta) \ \cos \overline{\omega} t \ \sin \tilde{\Omega} t, \quad (53)$$

where $\zeta = z_1\overline{R}/L$ and $\tilde{\Omega} = \Omega + \omega_0$ is the difference between the dominant frequencies in the moving frame of reference.

The solution (52, 53) indeed corresponds to the cycloidal oscillations of the vortex with the frequency $\overline{\omega}$, whose polarization rotates slowly with the frequency $\tilde{\Omega}$ in accordance with the phenomenological formula (29). It follows from this solution that for small values of R/L the amplitudes of the radial and azimuthal oscillations are approximately equal, linearly proportional to the radius of the gyrotropic rotation of the vortex and depend mainly on the ratio R/L. For small values of this parameter

$$a_r^{(max)} \simeq a_\chi^{(max)} \simeq \frac{1}{2z_1 c\sqrt{\beta}} \ \frac{R}{L} \ \simeq \ 1.24 \frac{R}{L}. \quad (54)$$

This result is in excellent agreement with the simulation data (see Tab. 1): from (54) it follows that the amplitudes of the principal modes are $\overline{a} = \overline{b} \simeq 0.62(R/L)$ (where $\overline{a} = a_r^{(max)}/2$, $\overline{b} = a_\chi^{(max)}/2$) which are close to the mean amplitudes $\overline{a} \simeq \overline{b} \simeq 0.6R/L$ from Table 1.

For larger R/L , $\overline{a}$ and $\overline{b}$ behave differently as functions of R/L, see Figure 5. This behavior is well explained by the functions $\zeta \mathrm{d}J_1(\zeta)/\mathrm{d}\zeta$ and $J_1(\zeta)$ in equations (52, 53). In fact, the agreement between these theoretical results and the simulation data is nearly perfect, as can be seen in Figure 5; only a factor of 1.03 was used for adjustment.

This agreement between the analytical and numerical results in the full interval of the values of R and L confirms our scenario for the origin of the cycloidal vortex oscillations.

5 Conclusion

In the frame of a 2D Heisenberg model with easy-plane symmetry we have studied the dynamics of a non-planar vortex on a circular system of radius L. Our simulations (numerical solution of the Landau-Lifshitz equations for the dynamics of spins on a square lattice with circular free boundaries) show the following main features of the vortex dynamics: In addition to the azimuthal rotation with radius R and angular velocity $\omega_0 = 1/(L^2 - R^2)$ the vortex performs small cycloidal oscillations around the mean trajectory showing a frequency doublet $\omega_{1,2}$, with mean value $\overline{\omega} \sim 1/L$ and splitting $\Delta\omega \simeq 4/L^2$. For small R/L the amplitudes of the radial and azimuthal componenets of the cycloidal oscillations both increase linearly with R/L, while they differ for large R/L, see Figure 5.

In contrast to an earlier *phenomenological* theory [15], which allowed to calculate $\omega_{1,2}$ for small R/L (but not the amplitudes), we have now given a *physical* explanation by the following scenario: The initial condition in a static vortex. When this vortex starts its motion under the influence of the Coulomb force from an image vortex and the gyrotropic force $\mathbf{G} \times \mathrm{d}\mathbf{R}/\mathrm{d}t$ it must excite two azimuthal magnon modes with nearly equal frequencies and amplitudes in order to compensate for its own angular momentum related to its azimuthal rotation. In the field of the oscillating and slowly rotating quasi-standing coherent spin wave the vortex performs its cysloidal oscillations around its mean trajectory. The amplitudes of these oscillations agree with an accuracy of about 3% with the simulation data for all R/L, which confirms the above scenario.

Finally we would like to stress that cycloidal vortex oscillations with two nearby frequencies are olso observed in simulations for other system shapes, *e.g.* for square systems, *i.e.* a circular system was only chosen here in order to allow analytical calculations.

One of us (A.S.K.) thanks the University of Bayreuth for kind hospitality and acknowledges finansial support from the Graduiertenkolleg "Nichtlineare Spektroskopie und Dynamik".

Appendix A

To explain the vortex dynamics we must calculate the integrals of motion, first of all the energy and angular momentum, which depend on the effective mass (21) of the vortex. All the calculations were performed for a small easy-plane anisotropy ($\delta = 0.1$). But even in this range the radius of the vortex core is very small ($r_v = 1.5$) and contains only a few spins. So we shall not discuss the contribution of the core to the integral characteristics of the vortex. For a moving vortex in the region outside the core the distribution of the fields has the form

$$m = m_0(r) + V m_1(\mathbf{r}), \quad \Phi = \varphi + V\Phi_1(\mathbf{r}), \tag{55}$$

where $m_0 \propto \Phi_1 \propto \exp(-r/r_v)$ and $m_1 \propto r_v/r$ (r and φ represent the polar coordinates in the frame connected with the vortex center). So the second term in (21) is exponentially small and can be omitted. Due to the small m-components we can use the relation (8) and rewrite the components of the mass tensor as

$$M_{ij} = \int \frac{\mathrm{d}v}{c^2} \frac{\partial\Phi}{\partial X_i} \frac{\partial\Phi}{\partial X_j}, \quad M_{ij}^{(0)} = \int \frac{\mathrm{d}v}{c^2} \frac{\partial\Phi}{\partial x_i} \frac{\partial\Phi}{\partial x_j}. \tag{56}$$

taking into account (M_{ij}) or not ($M_{ij}^{(0)}$) the boundary conditions as seen from (13).

Note that in this approximation an equation similar to (20) with M_{ii} from (56) can be derived from the ansatz $\mathbf{S} = \mathbf{S}(\mathbf{r}, \mathbf{R}(t))$ in a Lagrangian approach.

The energy (2) for the area out of the core can be simplified and expressed in terms of the mass components

$$\begin{aligned} E &\simeq \frac{1}{2} \int \mathrm{d}v \Big((\nabla\Phi)^2 + c^2 m^2 \Big) \\ &\simeq c^2 M^{(0)} + \frac{1}{2} M_{xx} \dot{X}^2 + \frac{1}{2} M_{yy} \dot{Y}^2, \end{aligned} \tag{57}$$

where $M^{(0)} = (M_{xx}^{(0)} + M_{yy}^{(0)})/2$.

The second integral of motion is the total angular momentum of the magnetization field [24]:

$$\mathbf{K} = \int \mathrm{d}v (1 - m) \Big[\mathbf{r} \times \nabla\Phi \Big]. \tag{58}$$

For the stationary gyrotropic rotation of a vortex the solution (13) has the form $\Phi = \chi + \tilde{\Phi}(r, R, \varphi - \chi)$ and a travelling wave ansatz is valid for the angle variable. So from (13) we have $\partial\Phi/\partial t = -\dot{\chi}(\partial\Phi/\partial\varphi - 1)$ and for the position of the vortex ($X = R$, $Y = 0$) the following relation is valid: $\partial\Phi/\partial\varphi - 1 = -R\,\partial\Phi/\partial Y$. Then it is easy to show that

$$\begin{aligned} K &= R^2 \dot{\chi} \frac{1}{c^2} \int \mathrm{d}v \left(\frac{\partial\Phi}{\partial Y} \right)^2 + \dot{\chi} r_v^2 \int \mathrm{d}v \left(\frac{\partial\Phi}{\partial\varphi} - 1 \right) \\ &\quad + (1 - m_0) \int \mathrm{d}v \frac{\partial\Phi}{\partial\varphi} \\ &= R^2 \dot{\chi} \Big(M_{\varphi\varphi} - \mu \Big) + (1 - m_0)\, \pi \Big(L^2 - R^2 \Big). \end{aligned} \tag{59}$$

In the chosen position of the vortex $M_{yy} = M_{\varphi\varphi}$. Besides we assumed that there exists a nonzero spatially uniform background with the magnetization m_0. The first term in (59) corresponds to the kinematic angular momentum

of the moving vortex and the second term to the angular momentum of a static vortex in the finite system.

In (59) the quantity μ represents the total z-component of the magnetization which is conserved in the uniaxial ferromagnet. For a static vortex only its interior part gives the contribution $\mu_0 \simeq \pi r_v^2$ to the magnetization which is the "self angular momentum" of the vortex (its total spin). But in a moving vortex the additional term $\delta m = \dot{\Phi}/c^2$ appears and the total magnetization is

$$\mu = \int \mathrm{d}v m = \mu_0 + \mu_0 RV, \tag{60}$$

where R and V are radius and velocity of the gyrotropic vortex motion.

We see that the mass M in the energy (57) and the angular momentum (59) plays the role of a usual particle mass.

For the calculation of the vortex mass we use the static solution (13) for a vortex on a circle with free boundary conditions and obtain the following results

$$M^{(0)}_{rr,\varphi\varphi} = \pi r_v^2 \left(\ln \frac{L}{r_v} + \ln(1-\varepsilon) \pm \frac{1}{2}\varepsilon \right), \tag{61}$$

$$M_{rr,\varphi\varphi} = \pi r_v^2 \left(\ln \frac{L}{r_v} + \frac{\varepsilon^2 \mp 2\varepsilon - 1}{2\varepsilon^2} \ln(1-\varepsilon) - \frac{1-2\varepsilon}{2\varepsilon} \mp 1 \right), \tag{62}$$

where $\varepsilon = (R/L)^2$.

So the rest energy of the vortex $c^2 M^{(0)}$ and its angular momentum are

$$E = \pi \ln \frac{L^2 - R^2}{L r_v}, \tag{63}$$

and

$$K = RV\pi r_v^2 \left(\ln \frac{L^2 - R^2}{L r_v} - \frac{(1-\varepsilon)^2}{2\varepsilon^2} \ln(1-\varepsilon) + 1 - \frac{1}{2\varepsilon} \right) + (1-m_0)\pi \left(L^2 - R^2 \right). \tag{64}$$

We can use the formulas (61–64) only in the region $L - R > r_v$ in which the omitted terms are negligibly small. So these formulas are accurate for all values of R in the interval $0 < R < L - r_v$. In the limit $R \to L$ all the expressions (61–64) logarithmically diverge due to the terms $\ln(1-\varepsilon)$ and the masses must be calculated with better accuracy. For small distance of the vortex from the boundary of the system (for a small value of the parameter $(L-R)/r_v \equiv l/r_v$) the boundary may be considered as a straight line along which the vortex moves. In this case the integrals in (56) can be expanded in a power series in $l/r_v \ll 1$ and the first terms of this expansion for the area outside the vortex core have the form

$$M_{out} \simeq \pi r_v^2 \left(\left(\frac{l}{r_v} \right)^2 + \frac{1}{3} \left(\frac{l}{r_v} \right)^6 + \ldots \right) \simeq \pi (L-R)^2, \tag{65}$$

and tend to zero near the boundary. In this region the core of the vortex gives the main contribution to its mass. But inside the vortex $m \simeq 1$ and $\partial\Phi/\partial\dot{Y} \sim (y - Y)$ (see [6]) (vortex moves along the surface in y-direction). So the contribution of the interior of the vortex to its mass is of order of the volume of the core: $\pi r_v^2/2 + 2r_v(L-R)$. Combining this estimate for $L - R < r_v$ with the formulas (61–62) for $L - R > r_v$ we can propose approximate expressions for the effective vortex masses valid for all radii of vortex rotation in which the logarithmic terms $\ln(1-\varepsilon)$ must be replaced by $\ln(1 - \varepsilon + r_v/L)$. In the limit $R \to L$ the amplitude of the m-field tends to zero and the vortex transforms into a small amplitude surface soliton with a stationary profile and a finite mass in the order of r_v^2. This solution was discussed in [26] (see also [27]).

Appendix B

In the simple case of a superposition of two principal modes with the same amplitude ($A_1 = A_2 = A$) the solution (38) has the form

$$\Phi_{sw}(\mathbf{r}, t) = A(P \sin\bar{\omega}t \cos(\varphi + \Omega t) + Q \cos\bar{\omega}t \sin(\varphi + \Omega t)), \tag{66}$$

where in the first approximation in the small parameter Ω

$$P \simeq J_1(\rho) + \frac{\pi\Omega}{4c^2} \left(Y_1(\rho) + \rho \frac{\mathrm{d}Y_1(\rho)}{\mathrm{d}\rho} \right) + \mathcal{O}(\Omega^2), \tag{67}$$

$$Q \simeq \frac{\pi\bar{\omega}}{4c^2} Y_1(\rho) + \frac{\Omega}{\bar{\omega}} \rho \frac{\mathrm{d}J_1(\rho)}{\mathrm{d}\rho} + \mathcal{O}(\Omega^2), \tag{68}$$

and $\rho = r z_1/L$.

The expression for the angular momentum of a coherent spin wave can be rewritten as

$$K_{sw} = -\frac{2\pi A^2}{c^2} \int_0^L r\mathrm{d}r \left(\Omega(P^2 + Q^2) + 2\bar{\omega}PQ \right) + \frac{2\pi A^2}{c^2} \int_0^L r\mathrm{d}r \Omega (P^2 - Q^2) \cos 2\bar{\omega}t, \tag{69}$$

and in the first approximation we have

$$K_{sw} \simeq -\frac{2\pi A^2 L^2}{c^2 z_1^2} \int_0^{z_1} \rho\mathrm{d}\rho ((J_1^2(\rho) + 2\rho J_1(\rho) \frac{\mathrm{d}J_1}{\mathrm{d}\rho} + \frac{\pi\bar{\omega}^2}{2c^2\Omega} J_1 Y_1) - \cos 2\bar{\omega}t\, J_1^2) + \mathcal{O}(\Omega^2). \tag{70}$$

From the expression in the first brackets in (70) it is evident that the shifts of the frequencies ω_i from their average value $\bar{\omega}$ in the arguments of the Bessel functions and the additional terms with Neumann functions in (38) give a contribution in K_{sw} of the same order as the main terms in (38). After performing the integrals in (70) we obtain the final result (43) if the last terms with Neumann functions in (38) are disregarded. The parameter α must be replaced by

$$\tilde{\alpha} = \frac{z_1^2+1}{2z_1^2} J_1^2(z_1) + \frac{z_1^2-1}{2z_1^2} J_1(z_1) Y_1(z_1) \simeq 0.11, \quad (71)$$

if these terms are taken into account.

References

1. A.A. Thiele, Phys. Rev. Lett. **30**, 230 (1973)
2. A.A. Thiele, J. Appl. Phys. **45**, 377 (1974)
3. D.L. Huber, Phys. Rev. B **26**, 3758 (1982)
4. A.M. Kosevich, V.P. Voronov, I.V. Manzhos, Sov. Phys. JETP **57**, 86 (1983)
5. A.V. Nikiforov, E.B. Sonin, Sov. Phys. JETP **58**, 373 (1983)
6. M.E. Gouvea, G.M. Wysin, A.R. Bishop, F.G. Mertens, Phys. Rev. B **39**, 11840 (1989)
7. G.M. Wysin, Phys. Rev. B **49**, 8780 (1994)
8. F.G. Mertens, G.M. Wysin, A.R. Völkel, A.R. Bishop, H.J. Schnitzer in *Nonlinear Coherent Structures in Physics and Biology*, edited by K.H. Spatschek, F.G. Mertens, NATO ASI Series B, Vol. 329 (Plenum Press, New York and London, 1994)
9. A.R. Völkel, G.M. Wysin, A.R. Bishop, F.G. Mertens, H.J. Schnitzer, Phys. Rev. B **50**, 12711 (1994)
10. G.M. Wysin, F.G. Mertens, A.R. Völkel, A.R. Bishop, in *Nonlinear Coherent Structures in Physics and Biology*, edited by K.H. Spatschek, F.G. Mertens, NATO ASI Series B, Vol. **329** (Plenum Press, New York and London, 1994)
11. G.M. Wysin, A.R. Völkel, Phys. Rev. B **52**, 7412 (1995)
12. G.M. Wysin, A.R. Völkel, Phys. Rev. B **54**, 12921 (1996)
13. G.M. Wysin, Phys. Rev. B **54**, 15156 (1996)
14. H.J. Schnitzer, Ph.D. thesis (in German), University of Bayreuth (1996)
15. F.G. Mertens, H.J. Schnitzer, A.R. Bishop, Phys. Rev. B **56**, 2510 (1997)
16. B.A. Ivanov, H.J. Schnitzer, F.G. Mertens, G.M. Wysin, Phys. Rev. B **58**, 8464 (1998)
17. G.M. Wysin, Phys. Lett. A **240**, 95 (1998)
18. T. Shinjo, T. Okuno, R. Hassdorf, K. Shigeto, T. Ono, Science **289**, 930 (2000)
19. J. Raabe, R. Pulwey, R. Suttler, T. Schweinbock, J. Zweck, D. Weiss, J. Appl. Phys. **88**, 4437 (2000)
20. M. Schneider, H. Hoffmann, J. Zweck, Appl. Phys. Lett. **77**, 2909 (2000)
21. R.P. Cowburn, D.K. Koltsov, A.O. Adeyeye, M.E. Welland, D.M. Tricker, Phys. Rev. Lett. **83**, (1999) 1042
22. T. Pokhil, D. Song, J. Nowak, J. Appl. Phys. **87**, 6319 (2000)
23. L.P. Pitaevskii, Sov. Phys. JETP **13**, 451 (1961)
24. A.M. Kosevich, B.A. Ivanov, A.S. Kovalev, Phys. Rep. **194**, 117 (1990)
25. B.A. Ivanov, A.K. Kolezhuk, G.M. Wysin, Phys. Rev. Lett. **76**, 511 (1996)
26. N. Papanicolaou, P.N. Spathis, Nonlinearity **12**, 285 (1999)
27. A.S. Kovalev, E.S. Syrkin, G.A. Maugin, Low Temp. Phys. **28**, 452 (2002)